

Supporting Information

Murata and Tanaka 10.1073/pnas.1501149112

SI Text

Analysis of Locally Favored Structures. We assumed the locally favored structures to have nearly spherical shape with rough interface. Because we obtain $d_f \sim 2.3 < 3$, it is worth considering a different possibility for the shape of a LFS. Here we check a case where the LFS has a 2D disk-like shape. Note that a decoupling approximation for $F(q)$ (1) is used by assuming an anisotropic disk-like shape for $P(q)$. Accordingly, we obtain a fitting as good as that of the fractal cluster model. However, the radius of the disk and its thickness are estimated as 3.6 and 0.06 nm, respectively. The value of $d = 0.06$ nm is less than the size of one molecule, which is unphysical. Thus, we conclude that a complex shape of the LFS is the most reasonable interpretation.

Formation and Growth of Microcrystallites During LLT. Here we consider how microcrystallites are formed during LLT (2, 3), focusing on the following two problems: (i) why there is the radial symmetry of microcrystal orientation in droplets of liquid II formed in nucleation-growth (NG)-type LLT, which causes Maltese cross patterns in polarizing microscopy observation (2) and four-leaf depolarized scattering patterns in light-scattering experiments (3), and (ii) why microcrystallites do not keep growing in size after their formation. First we focus on problem (i). In our previous study (4), we found that liquid II is more wettable to crystals than liquid I, implying a lower nucleation barrier ΔG for crystal nucleation in liquid II than in liquid I. On the other hand, the molecular mobility μ is much higher in liquid I than in liquid

II. Note that T_a is in the glass-transition region of liquid II but above that of liquid I (5, 6), implying that liquid II formed in NG-type LLT is in a glassy state. Thus, the nucleation probability, which is proportional to $\mu \exp(-\Delta G/(k_B T))$ (k_B being Boltzmann's constant), should be maximum at the liquid I–liquid II interface. Furthermore, the growth should be easier in a direction perpendicular to the interface toward the liquid I side because of much larger μ there. We speculate that this coupling between the liquid I–liquid II interface and the crystal growth direction is the origin of the radial symmetry. Now we consider problem (ii). The growth of microcrystallites is suppressed by slow dynamics associated with the glass transition of liquid II immediately after the transformation from liquid I to glassy liquid II. NG-type ordering leads to a discontinuous change from liquid I to liquid II, which results in a discontinuous drop of μ . The faster growth of glassy liquid II than the crystal (5) leads to immediate inclusion of the latter in the former, preventing further growth of the crystals. This scenario also indicates that the amount of microcrystallites should steeply decrease below T_{SD} because (i) there is no mechanism to rapidly lower ΔG for SD-type LLT, where the order parameter changes only continuously, and (ii) the mobility is very low even for liquid I because T_a becomes closer to T_g of liquid I. This is consistent with the decrease of the scattering from microcrystallites at lower T_a (Fig. 2) and our previous estimation of the amount of microcrystallites (5). Because the discussion here is speculative, the above scenario is to be confirmed carefully in the future.

1. Kotlarchyk M, Chen SH (1983) Analysis of small angle neutron scattering spectra from polydisperse interacting colloids. *J Chem Phys* 79(5):2461–2469.
2. Tanaka H (2013) Importance of many-body orientational correlations in the physical description of liquids. *Faraday Discuss* 167:9–76.
3. Shimizu R, Kobayashi M, Tanaka H (2014) Evidence of liquid-liquid transition in triphenyl phosphite from time-resolved light scattering experiments. *Phys Rev Lett* 112(12):125702.
4. Murata K, Tanaka H (2010) Surface-wetting effects on the liquid-liquid transition of a single-component molecular liquid. *Nat Commun* 1:16.
5. Tanaka H, Kurita R, Mataka H (2004) Liquid-liquid transition in the molecular liquid triphenyl phosphite. *Phys Rev Lett* 92(2):025701.
6. Kurita R, Tanaka H (2005) Control of the fragility of a glass-forming liquid using the liquid-liquid phase transition. *Phys Rev Lett* 95(6):065701.

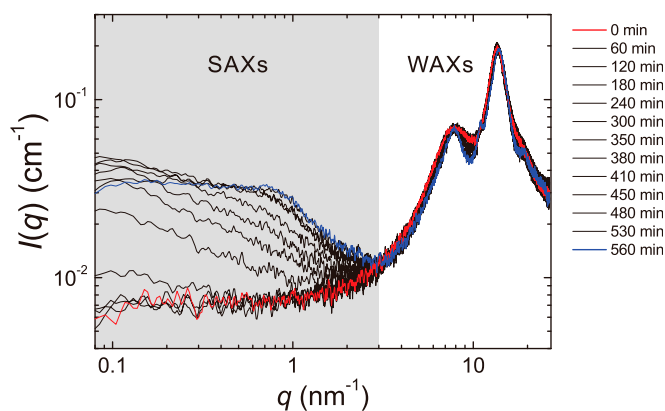


Fig. S1. Time evolution of smeared scattering function $I(q)$ during LLT at $T_a = 212$ K obtained by time-resolved small- and wide-angle X-ray scattering (SWAXs). The red and blue solid lines correspond to $I(q)$ at 0 min (liquid I) and 560 min (liquid II), respectively. The black solid lines indicate $I(q)$ in the transformation process. The gray regime shows the scattering at small angles.

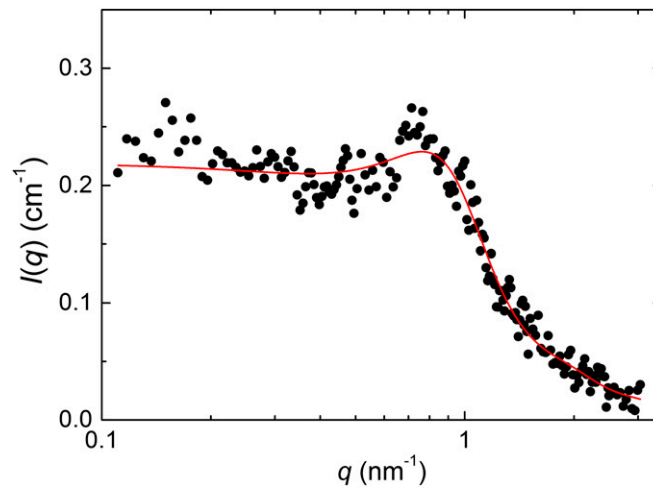


Fig. S2. $I(q)$ in a small-angle regime at $T_a = 212$ K, observed after the transformation (at 560 min). Here the contribution from wide-angle scattering (the tail of the peak at $q = 7.7 \text{ nm}^{-1}$ is already subtracted from the original data. We can see a shallow dip around $q = 0.7 \text{ nm}^{-1}$. The red solid curve represents the best fits by Eqs. 3–5.

Table S1. T_a -dependence of the characteristics of LFS and microcrystallites

T_a (K)	212	213	214	216	218
R_g , nm	3.0	3.0	2.9	3.0	3.0
d_f	2.2	2.5	2.4	2.2	2.4
$I_{\text{LFS}}(0)$, cm^{-1}	0.17	0.17	0.18	0.17	0.18
ϕ_{LFS}	0.15	0.17	0.14	0.14	0.16
ϕ_{MC}	0.11	0.092	0.12	0.15	0.16

T_a dependences of the gyration radius, R_g , the mass fractal dimension, d_f , the prefactor, $I_{\text{LFS}}(0)$, the volume fraction estimated from the Percus–Yevick equation, ϕ_{LFS} , and the area fraction of peak II, ϕ_{MC} .